

Kinetic Characterization of the GTPase Activity of Phage λ Terminase: Evidence for Communication between the Two “NTPase” Catalytic Sites of the Enzyme[†]

Liping Woods[‡] and Carlos Enrique Catalano^{*,‡,§}

Department of Pharmaceutical Sciences and Molecular Biology Program, University of Colorado Health Sciences Center, Denver, Colorado 80262

Received April 14, 1999

ABSTRACT: The terminase enzyme from bacteriophage λ is responsible for the insertion of viral DNA into the confined space within the capsid. The enzyme is composed of the virally encoded proteins gpA (73.3 kDa) and gpNu1 (20.4 kDa) isolated as a gpA₁·gpNu1₂ holoenzyme complex. Lambda terminase possesses a site-specific nuclease activity, an ATP-dependent DNA strand-separation activity, and an ATPase activity that must work in concert to effect genome packaging. We have previously characterized the ATPase activity of the holoenzyme and have identified catalytic active sites in each enzyme subunit [Tomka and Catalano (1993) *Biochemistry* 32, 11992–11997; Hwang et al. (1996) *Biochemistry* 35, 2796–2803]. We have noted that GTP stimulates the ATPase activity of the enzyme, and terminase-mediated GTP hydrolysis has been observed. The studies presented here describe a kinetic analysis of the GTPase activity of λ terminase. GTP hydrolysis by the enzyme requires divalent metal, is optimal at alkaline pH, and is strongly inhibited by salt. Interestingly, while GTP can bind to the enzyme in the absence of DNA, GTP hydrolysis is strictly dependent on the presence of polynucleotide. Unlike ATP hydrolysis that occurs at both subunits of the holoenzyme, a single catalytic site is observed in the steady-state kinetic analysis of GTPase activity ($k_{\text{cat}} \approx 37 \text{ min}^{-1}$; $K_m \approx 500 \text{ } \mu\text{M}$). Moreover, while GTP stimulates ATP hydrolysis (apparent $K_D \approx 135 \text{ } \mu\text{M}$ for GTP binding), all of the adenosine nucleotides examined strongly inhibit the GTPase activity of the enzyme. The data presented here suggest that the two “NTPase” catalytic sites in terminase holoenzyme communicate, and we propose a model describing allosteric interactions between the two sites. The biological significance of this interaction with respect to the assembly and disassembly of the multiple nucleoprotein packaging complexes required for virus assembly is discussed.

The terminase enzyme from bacteriophage λ is required for the assembly of an infectious viral particle from empty, performed procapsids and a concatemeric DNA substrate made up of multiple viral genomes linked in a linear array (see Figure 1) (1–4). Phage λ terminase is composed of two virally encoded proteins, gpNu1¹ (20.4 kDa) and gpA (73.3 kDa), in a gpA₁·gpNu1₂ holoenzyme complex that forms, at least in part, a molecular “machine” whose role is to excise a single genome from the concatemer and insert it into the

confined space within the viral capsid (1, 3, 5). The holoenzyme possesses site-specific endonuclease, strand-separation, and ATPase catalytic activities that work in concert to effect DNA packaging (1, 3, 4). ATP modulates several aspects of the packaging pathway (Figure 1) including the assembly of the terminase subunits onto DNA and the stability of the resulting nucleoprotein packaging complexes (6, 7). ATP also affects the nuclease activity of the enzyme, increasing the rate of the reaction and ensuring that the duplex is nicked appropriately to form the 12 base single-stranded “sticky” end of the mature viral genome (8–10). These studies suggest that ATP is required for the assembly of a catalytically competent nuclease complex of high fidelity. ATP hydrolysis is further required to separate the nicked, annealed strands formed by the nuclease activity of the enzyme, and it is presumed that terminase translocation during active DNA packaging is driven by the hydrolysis of ATP (1–4).

We have previously examined the nuclease (5, 11), strand-separation (12), and ATPase (13, 14) catalytic activities of λ terminase in order to more clearly define the kinetic parameters that govern these reactions, and to investigate catalytic interactions that are required to effect DNA packaging. With respect to the ATPase activity of the enzyme, we have demonstrated that both enzyme subunits possess a DNA-stimulated ATPase catalytic site, a high-affinity (K_m

[†] This work was supported by National Institutes of Health Grant GM50328-04.

* Address correspondence to this author at the School of Pharmacy, C238, University of Colorado Health Sciences Center, 4200 E. Ninth Ave., Denver, CO 80262. (303) 315-8561 (phone), (303) 315-6281 (fax), carlos.catalano@uchsc.edu (e-mail).

[‡] Department of Pharmaceutical Sciences, School of Pharmacy, UCHSC.

[§] Molecular Biology Program, School of Medicine, UCHSC.

¹ Abbreviations: AXP, term used to describe adenosine nucleotides used in this study, including ATP, dATP, and ADP; bp, base pair(s); β -ME, 2-mercaptoethanol; *cos*, cohesive end site, the junction between individual genomes in immature concatemeric λ DNA; *cos*-cleavage reaction, the site-specific endonuclease activity of λ terminase; gpA, the large subunit of phage λ terminase; gpNu1, the small subunit of phage λ terminase; IHF, *E. coli* integration host factor; kb, kilobase(s); kDa, kilodalton(s); NTPase activity, an ATPase and/or GTPase catalytic activity; GXP, term used to describe guanosine nucleotides used in this study, including GTP, dGTP, GDP, and dGDP; PAGE, polyacrylamide gel electrophoresis.

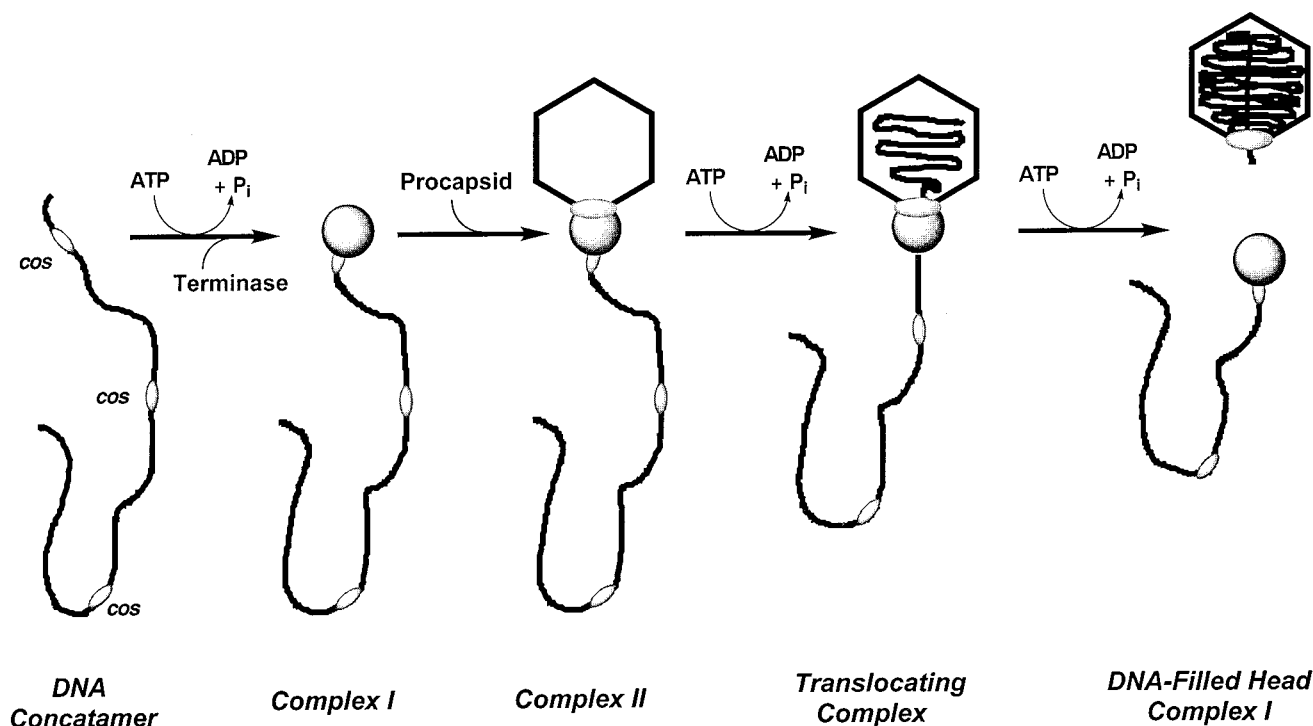


FIGURE 1: Model for DNA packaging by phage λ terminase.

$\approx 5 \mu\text{M}$) site in gpA and a low-affinity ($K_m \approx 470 \mu\text{M}$ in the presence of DNA) site in the smaller gpNu1 subunit of the holoenzyme (13–15). These studies have also demonstrated that GTP and dGTP stimulate the ATPase activity of the enzyme (13), and terminase-mediated GTP hydrolysis has been demonstrated (16).

Here, we present a kinetic analysis of the GTPase activity of phage λ terminase in order to clarify the role of this catalytic activity in the packaging of viral DNA. Surprisingly, our data demonstrate that the catalytic requirements for ATP and GTP hydrolysis by the enzyme are distinctly different. Moreover, unlike ATP hydrolysis where two catalytic sites are observed, a kinetic analysis of GTP hydrolysis reveals a single catalytic site. Finally, our data strongly suggest that the two “NTPase” catalytic sites communicate, and we suggest that this interaction is important in the assembly and function of the terminase DNA packaging machine.

EXPERIMENTAL PROCEDURES

Materials. Radiolabeled nucleotides were purchased from Amersham–Pharmacia. Unlabeled nucleotides were purchased from Boehringer Mannheim Biochemicals. Restriction endonucleases were purchased from Life Technologies. All divalent metals were purchased from Mallinckrodt as dichloride salts. Spermidine and ampicillin were purchased from Sigma Chemical Co. Silica TLC plates were purchased from J. T. Baker. All other materials were of the highest quality commercially available.

Bacterial Strains, DNA Preparation, and Protein Purification. Purification of terminase holoenzyme and the isolated gpA and gpNu1 subunits was performed as previously described (5, 17). *E. coli* integration host factor was purified from the overexpressing strain HN880 (generously provided by H. Nash, National Institutes of Health, Bethesda, MD) by the method of Nash et al. (18). All of our purified proteins were homogeneous as determined by SDS–PAGE and

densitometric analysis using a Molecular Dynamics laser densitometer and the ImageQuant data analysis package. Unless otherwise indicated, the concentration of catalytically active terminase (holoenzyme and reconstituted enzyme) was determined by active-site titration experiments as described previously (5). The *cos*-containing plasmid pAFP1, kindly provided by M. Feiss (University of Iowa, Iowa City, IA), was purified from the *E. coli* strain JM107[pAFP1] using Qiagen DNA prep columns. The *cos*-containing 266_{mer} DNA duplex and the 216_{mer} duplex of random sequence were prepared starting with pAFP1 as described previously (19).

Activity Assays. The standard *GTPase* reaction mixtures (10 μL) contained 20 mM Tris–HCl buffer (pH 9.0), 10 mM MgCl_2 , 2 mM spermidine, 7 mM $\beta\text{-ME}$, 2.5 μM [$\alpha\text{-}^{32}\text{P}$]GTP, *ScaI*-linearized pAFP1 (25 nM duplex, 72 μM base pairs), and, unless otherwise indicated, 100 nM λ terminase. The reaction was initiated with the addition of enzyme and allowed to proceed at 37 °C. Aliquots (2 μL) were removed at the indicated times, and the reaction was stopped with the addition of an equal volume of 100 mM EDTA. The quenched reaction mixture (2 μL) was spotted on a silica gel TLC plate which was developed twice with buffer A (125 mL of 2-propanol, 60 mL of NH_4OH , 15 mL of water). GDP formation was quantitated using a Molecular Dynamics Phosphorimaging system and the ImageQuant software package. The *ATPase* activity assays (10 μL) contained 20 mM Tris–HCl buffer (pH 9.0), 10 mM MgCl_2 , 2 mM spermidine, 7 mM $\beta\text{-ME}$, 100 nM terminase, and, unless otherwise indicated, 1 mM [$\alpha\text{-}^{32}\text{P}$]ATP. The reaction was initiated with the addition of enzyme, and the reaction was allowed to proceed at 37 °C. Aliquots (2 μL) were removed at the indicated times, and the reaction was stopped with the addition of an equal volume of 100 mM EDTA. Quantitation of ADP formation was performed as described above in the GTP assay. The *cos*-cleavage assay (25 μL) contained 20 mM Tris–HCl buffer (pH 8), 10 mM MgCl_2 , 2

mM spermidine, 7 mM β -ME, 1 mM ATP, and 200 nM terminase. Unless otherwise indicated, the DNA substrate was *ScaI*-linearized pAFP1, a 2897 bp *cos*-containing plasmid (20), that was included at a concentration of 50 nM (duplex) with an equal molar concentration of IHF. The reaction was initiated with the addition of enzyme, and the reaction was allowed to proceed at 37 °C. Aliquots (3 μ L) were removed at the indicated times, and the reaction was stopped with the addition of an equal volume of 100 mM EDTA. The DNA was fractionated by a 0.6% agarose gel, and the ethidium bromide-stained products were analyzed by video densitometry as previously described (5). The raw data were quantitated using the Molecular Dynamics Image-Quant software package (5, 11).

Kinetic Analysis. The kinetic constants for steady-state GTP hydrolysis (Figure 3) were determined by nonlinear regression analysis of the data based on the equation:

$$k_{\text{obs}} = \frac{k_{\text{cat}}[\text{GTP}]}{K_{\text{m}} + [\text{GTP}]} \quad (1)$$

where k_{obs} is the rate of GDP formation (min^{-1}) at a given concentration of GTP. The rate of GDP formation (nM/min) was determined from a full reaction time course, and only those data within the linear portion of the reaction curve were used. This rate was converted to k_{obs} by dividing by the concentration of enzyme used in the assay. Regression analysis was performed using the Igor data analysis program (Wave Metrics, Lake Oswego, OR).

Analysis of GTP-mediated stimulation of ATP hydrolysis (Figure 4) was determined using the equation:

$$k_{\text{obs}} = k_0 + \frac{k_{\text{max}}[\text{GTP}]}{K_{\text{D,app}} + [\text{GTP}]} \quad (2)$$

where k_0 is the rate of ATP hydrolysis in the absence of GTP, k_{obs} is the rate of ATP hydrolysis at a given concentration of GTP, k_{max} is the rate of ATP hydrolysis at infinite GTP concentration, and $K_{\text{D,app}}$ is the apparent binding constant for GTP. Nonlinear regression analysis was performed using the Igor data analysis program.

RESULTS

Optimization of the GTPase Reaction Conditions. We have previously examined the ATPase activity of λ terminase and optimized this reaction with respect to buffer pH, salt concentration, and the requirement for divalent metal (13). We present here similar studies on the GTPase activity of the enzyme. GTP hydrolysis by the enzyme is optimal at alkaline pH (not shown) with a pH–rate profile similar to that observed for ATP hydrolysis (13) and *cos*-cleavage activities (5). Consistent with the ATPase (13, 16), nuclease (5, 21), and strand-separation (12, 16) catalytic activities of the enzyme, divalent metal is strictly required for GTP hydrolysis (Table 1); however, differences in the metal requirement for terminase-mediated ATP and GTP hydrolysis are notable as follows. (i) Maximal GTPase activity is observed at a Mg^{2+} concentration of 5 mM (not shown), significantly greater than that observed for terminase-

Table 1: Divalent Metal Requirement for GTP Hydrolysis^a

divalent metal	relative GTPase act.	divalent metal	relative GTPase act.
none	ND*	Ba^{2+}	4 ± 0.5
Mg^{2+}	100	Cd^{2+}	2 ± 0.1
Mn^{2+}	72 ± 11	Co^{2+}	2 ± 0.2
Ca^{2+}	18 ± 5	Cu^{2+}	2 ± 0.5
Sr^{2+}	4 ± 1	Zn^{2+}	1 ± 0.1

^a The GTPase activity assay was conducted as described under Experimental Procedures except that the terminase concentration was increased to 400 nM. Each divalent metal (as the chloride salt) was added to a final concentration of 5 mM. 100% relative activity represents 1.7 μ M GDP formed in 30 min. Each value represents the average of two individual experiments with errors indicating the variation between the experiments. ND, not detectable, <1%. We note that neither Zn^{2+} nor Cu^{2+} supports GTPase (above), ATPase (13), nuclease (5), or strand-separation (12) activities of the enzyme. This may reflect denaturation of the protein by these metals rather than an inherent inability to support catalysis.

mediated ATP hydrolysis (1.5 mM) (13).² (ii) While significant ATPase activity is observed at Mg^{2+} concentrations up to 25 mM (13), inhibition of GTP hydrolysis occurs at elevated concentrations of Mg^{2+} (not shown). (iii) Significant GTP hydrolysis is observed only in the presence of Mg^{2+} , Mn^{2+} , and Ca^{2+} , with minimal activity observed with any of the other metals tested (Table 1). This metal selectivity closely resembles that observed for the nuclease activity of the enzyme (5), but surprisingly differs from the promiscuous nature of the metal-dependent ATPase activity (13). Differences between the two NTPase activities are also observed in the salt effects on the reaction. While salt stimulates terminase-mediated ATP hydrolysis [maximal stimulation at 200 mM NaCl (13)], the GTPase activity of the enzyme is strongly inhibited by salt and is negligible at 200 mM NaCl (not shown).

GTPase Activity Is DNA-Dependent. We (13, 14) and others (16) have demonstrated that the ATPase activity of phage λ terminase is stimulated by DNA. Figure 2 demonstrates that the GTPase activity of the enzyme is strictly dependent on DNA, and no detectable GDP formation is observed in its absence. The stoichiometric binding data presented in Figure 2 suggest that 1–2 nM duplex DNA maximally stimulates GTP hydrolysis by the enzyme, and analysis of the data yields an equivalence point of $\approx 1.2 \pm 0.1$ nM duplex. This is significantly lower than the enzyme concentration (100 nM), suggesting that (i) each duplex can bind multiple terminase enzymes and that (ii) an intact *cos*-site is not required to promote GTP hydrolysis. This is supported by the observation that nonspecific DNA is as effective as *cos*-containing DNA in supporting GTPase activity (not shown).

² We note that while the concentration of GTP is 400-fold less than that of ATP (2.5 μ M vs 1 mM), higher concentrations of Mg^{2+} are required for optimal GTPase activity. Thus, the different metal concentrations required for optimal activity cannot be ascribed to the formation of a Mg^{2+} -nucleotide chelate required for catalysis. Moreover, metal chelation by DNA included in the GTPase assay (but not in the ATPase assay) might be expected to decrease the concentration of free Mg^{2+} ; however, if one assumes that each nucleotide in the duplex chelates one divalent metal (it is undoubtedly less than this), a 2987 bp duplex (pAFP1) at a concentration of 25 nM would chelate ≈ 75 μ M metal. This is insufficient to account for the observed 3.5 mM difference in optimal activity between the two reactions.

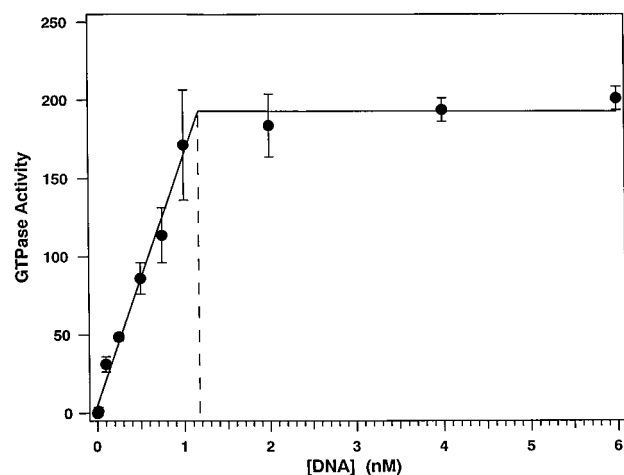


FIGURE 2: GTPase activity is DNA-dependent. The GTPase assay was performed as described under Experimental Procedures, except that the indicated concentration of DNA (*ScaI*-linearized pAFPI) was included. GTPase activity refers to the amount of GDP (nM) formed in 20 min. Each data point represents the average of two experiments with errors indicating the variation between the experiments. The dashed line indicates the equivalence point.

We have previously demonstrated that terminase binds to DNA in the nanomolar concentration range (19, 22). Assuming that the enzyme is fully active and that DNA binds to a single site on the enzyme, these data may be used to estimate the size of the DNA duplex required to promote GTP hydrolysis:

$$\text{site size} = \frac{(1.2 \text{ nM duplex})(2897 \text{ bp/duplex})}{100 \text{ nM enzyme}} \approx 35 \text{ bp/binding site}$$

We note that this binding site size is comparable to the gpNu1 DNA recognition elements, or R-elements (16 bp) (23).

GTP Hydrolysis by the Isolated Terminase Subunits. We have previously demonstrated that the isolated gpNu1 subunit possesses little, if any, ATPase activity and that full expression of catalytic activity requires interactions with gpA (15). Similar results were observed for the GTPase activity of the enzyme (not shown). We note, however, that GTP hydrolysis by gpNu1 under these experimental conditions is slightly greater than that observed for ATP hydrolysis by this subunit. Moreover, GTP hydrolysis by each subunit, as well as the reconstituted enzyme, is strictly dependent on the presence of DNA (not shown).

Effect of Nucleotides on GTPase Activity. Table 2 shows the effects of other nucleotides on the GTPase activity of terminase. Initial experiments utilized 2.5 μM radiolabeled GTP substrate while cold nucleotides were included at 10 μM . Under these conditions, the products of the GTP hydrolysis reaction (GDP and PO_4^{2-}) do not significantly affect GTPase activity, even though they are present at 4-fold excess over the radiolabeled substrate. Surprisingly, while guanosine nucleotides significantly stimulate the ATPase activity of the enzyme (see Table 4) (13), all of the adenosine nucleotides (AXP) strongly inhibit terminase-mediated GTP hydrolysis (Table 2). To explore this further, we repeated the experiment using significantly greater concentrations of radiolabeled GTP (1 mM), but keeping the concentration of

Table 2: Nucleotide Effects on GTP Hydrolysis^a

$[\alpha\text{-}^{32}\text{P}]\text{GTP}$	nucleotide added	relative GTPase activity
2.5 μM	none	100*
2.5 μM	GDP	105 \pm 3
2.5 μM	PO_4^{2-}	98 \pm 2
2.5 μM	ADP	46 \pm 1
2.5 μM	UTP	110 \pm 11
2.5 μM	CTP	125 \pm 8
2.5 μM	ATP	47 \pm 1
2.5 μM	dTTP	114 \pm 7
2.5 μM	dCTP	139 \pm 11
2.5 μM	dGTP	110 \pm 15
2.5 μM	dATP	47 \pm 6
1 mM	none	100*
1 mM	ATP	63 \pm 2
1 mM	ADP	60 \pm 4
1 mM	GDP	103 \pm 3

^a The GTPase activity assay was conducted as described under Experimental Procedures using the indicated concentration of $[\alpha\text{-}^{32}\text{P}]\text{GTP}$ and in the presence of 10 μM cold nucleotide as indicated. Each value represents the average of two experiments with errors indicating the variation between the experiments.

cold nucleotide at 10 μM . Under these experimental conditions, it is unlikely that AXP would compete for GTP binding as it is present at a 100-fold lower concentration. Again, GDP has little effect on GTP hydrolysis and, remarkably, all of the adenosine nucleotides continue to inhibit GTP hydrolysis (Table 2). Given the disparate concentrations of nucleotides used, these data suggest that the two purine nucleotides bind to discrete sites on the enzyme. Moreover, that 10 μM AXP is sufficient to significantly inhibit the reaction suggests that interactions with the high-affinity ATP-binding site found in the gpA subunit ($K_m = 5 \mu\text{M}$) are responsible for the observed inhibition of GTPase activity.

Kinetic Analysis of GTP Hydrolysis. We have previously characterized the steady-state ATPase activity of λ terminase and have identified two catalytic sites in the enzyme: a high-affinity ($K_m = 5 \mu\text{M}$) site in gpA, and a low-affinity ($K_m = 470 \mu\text{M}$) site in the gpNu1 subunit of the enzyme (13, 14). A steady-state kinetic analysis of terminase-mediated GTP hydrolysis is presented in Figure 3 and, unlike the ATPase activity of the enzyme, no evidence for multiple GTPase catalytic sites is obtained. These data are well-described by a single hyperbolic curve function yielding k_{cat} and K_m values of $37 \pm 2 \text{ min}^{-1}$ and $500 \pm 125 \mu\text{M}$, respectively.

Effect of Guanosine Nucleotides on *cos*-Cleavage Activity. It has previously been demonstrated that ATP stimulates the nuclease (*cos*-cleavage) activity of λ terminase (8, 10, 24) and that GTP modestly affects the reaction (21). We have confirmed these results and have further demonstrated that ADP and GDP also stimulate the *cos*-cleavage reaction (Table 3). Interestingly, the observed stimulation by nucleoside diphosphates is additive.

Effect of Guanosine Nucleotides on ATPase Activity. We have previously demonstrated that GTP and dGTP stimulate ATP hydrolysis by λ terminase (13), and Table 4 shows that GDP is equally effective. Importantly, a concentration of 2.5 mM GXP significantly stimulates the hydrolysis of ATP present at a concentration of 25 μM , again suggesting that the two nucleotides are interacting at discrete sites on the enzyme. Figure 4 shows the effect of GTP concentration on the observed rate of ATP hydrolysis by the enzyme, and

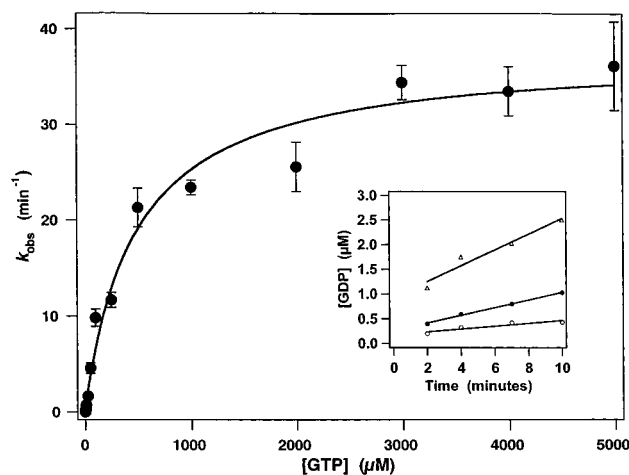


FIGURE 3: Kinetic analysis of terminase GTPase activity. The GTPase assay was performed as described under Experimental Procedures except that the concentration of $[\alpha\text{-}^{32}\text{P}]\text{GTP}$ was as indicated in the figure. Each data point represents the average of two separate experiments, and the solid line represents the best fit of the data to a single hyperbolic curve function as described. Inset: GDP formation in the presence of (○) 5 μM GTP, (●) 10 μM GTP, and (△) 25 μM GTP. Similar time courses were obtained in experiments where the reaction was initiated with the addition of Mg^{2+} (not shown).

Table 3: Nucleotide Effects on Terminase *cos*-Cleavage Activity^a

nucleotide added	rel nuclease act.	nucleotide added	rel nuclease act.
none	100*	GDP	127 ± 1
ATP	139 ± 3	ATP + GTP	144 ± 1
ADP	125 ± 1	ADP + GDP	160 ± 4
GTP	111 ± 3		

^a The *cos*-cleavage assay was conducted as described under Experimental Procedures except that the indicated nucleotides were added at a concentration of 1 mM. 100* relative activity represents 21 nM DNA products formed at 40 min. Each value represents the average of two experiments with errors indicating the variation between the experiments.

Table 4: Guanosine Nucleotides Stimulate ATPase Activity^a

additions	relative ATPase activity (25 μM $[\alpha\text{-}^{32}\text{P}]\text{ATP}$)	relative ATP hydrolysis (1 mM $[\alpha\text{-}^{32}\text{P}]\text{ATP}$)
none	100	100
GTP	139 ± 2	148 ± 15
GDP	142 ± 2	152 ± 12
dGTP	—	140*
DNA	257 ± 4	470 ± 7

^a The ATPase activity assay was conducted as described under Experimental Procedures using the indicated concentrations of $[\alpha\text{-}^{32}\text{P}]\text{ATP}$ substrate. Guanosine nucleotides (cold) were added at a concentration of 2.5 mM, and DNA was added at a concentration of 25 nM as indicated in the table. Each value represents the average of two experiments with errors indicating the variation between the experiments. (*) Cold dGTP was included at 5 mM (data taken from ref 13).

analysis of the data yields an apparent binding constant of $136 \pm 16 \mu\text{M}$ for GTP. We note that this experiment was performed in the absence of DNA, conditions where GTP hydrolysis does not occur (see Figure 2).

DISCUSSION

The terminase enzyme from bacteriophage λ is responsible for the packaging of viral DNA into the confined space within the viral capsid. The enzyme possesses site-specific

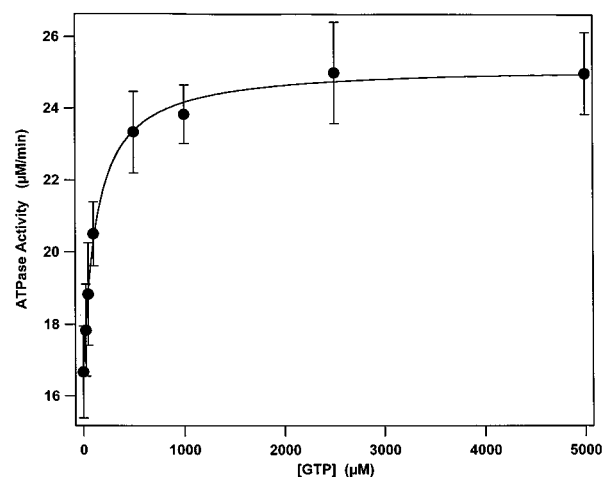
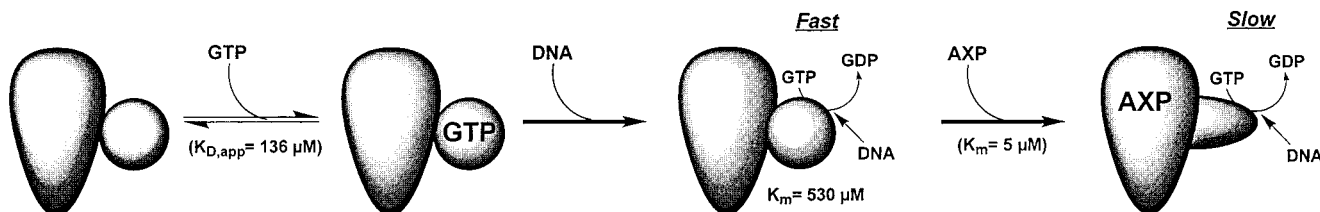


FIGURE 4: GTP stimulates ATPase activity. The ATPase assay was conducted as described under Experimental Procedures except that the indicated concentration of GTP was added to the reaction mixture. Each data point represents the average of three separate experiments, and error bars indicate one standard error about the mean. The solid line represents the best fit of the data to a hyperbolic curve function as described under Experimental Procedures.

endonuclease, strand-separation, and ATPase catalytic activities that work in concert to effect virus assembly (1–3). These activities have been examined in several laboratories (5, 11–14, 16, 21, 25), and we have previously performed kinetic analyses of each of these reactions (5, 11–14). With respect to the ATPase activity of the enzyme, the data from our studies were consistent with a simple two binding site model describing independent, noninteracting ATPase catalytic sites (13). More complex models involving allosteric regulation and interaction between the two catalytic sites were considered, but our original data did not allow us to kinetically distinguish them from the simple model. Mutagenesis studies have confirmed that both of the subunits in the holoenzyme hydrolyze ATP with high-affinity ($K_m = 5 \mu\text{M}$) and low-affinity ($K_m = 470 \mu\text{M}$) catalytic sites located in the gpA and gpNu1 subunits, respectively (14). We have previously shown that GTP stimulates ATP hydrolysis by the enzyme (13), and a terminase GTPase activity has been demonstrated (16). In the work presented here, we have characterized this GTPase activity and have compared the reaction parameters to those observed for ATP hydrolysis by the enzyme.

Given the obvious similarities in ATP and GTP hydrolysis reactions, we anticipated that the ATPase and GTPase activities of λ terminase would be quite similar. While some aspects are indeed similar, important differences between the two reactions were immediately apparent. First, although both reactions show a strict requirement for divalent metal, GTPase activity is supported by a much more limited range of metals than is ATP hydrolysis (13). Second, while the ATPase activity of the enzyme is stimulated by DNA (13), GTP hydrolysis is strictly dependent on the presence of polynucleotide. Third, while salt stimulates terminase-mediated ATP hydrolysis, GTPase activity is strongly inhibited by both sodium chloride and potassium glutamate. This is easily understood, however, as salt inhibits DNA binding by the enzyme (19) which likely indirectly inhibits the DNA-dependent GTPase activity. Finally, unlike ATP hydrolysis which occurs at both subunits of the holoenzyme

A. GTPase Activity



B. ATPase Activity

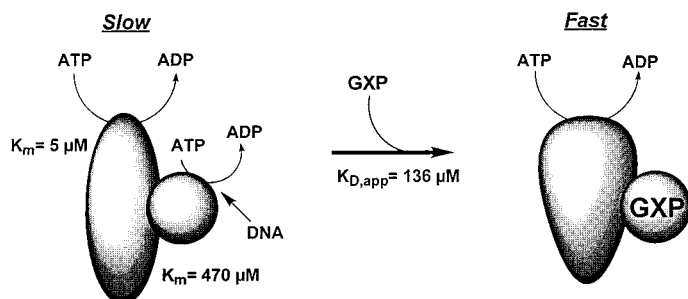


FIGURE 5: Model for interacting NTPase catalytic sites in phage λ terminase.

(13, 14), a single catalytic site is observed in the steady-state kinetic analysis of GTPase activity, suggesting that GTP hydrolysis occurs in only one of the enzyme subunits.³

Further differences between the two catalytic activities surfaced when we examined the effect of each nucleotide on the hydrolysis of the other. Strikingly, while guanosine nucleotides stimulate terminase-mediated ATP hydrolysis, adenosine nucleotides *inhibit* the GTPase activity of the enzyme. The data presented here strongly suggest that these interactions result from the two nucleotides binding to discrete, but interacting sites in the holoenzyme complex. First, 10 μM AXP is sufficient to significantly inhibit the hydrolysis of GTP present at a concentration of 1 mM . Given that AXP is present at 100-fold lower concentrations, it is unlikely that this inhibition results from direct competition for a single NTP binding site. Rather, the data suggest that AXP interactions with a high-affinity binding site negatively regulate GTP hydrolysis at a discrete GTPase catalytic site. Second, guanosine nucleotides present at 2.5 mM *stimulate* the hydrolysis of ATP present at a concentration of 25 μM . These data suggest that ATP hydrolysis occurs at a high-affinity ATPase catalytic site, and that the activity of this site is positively regulated by GXP binding to a separate site in the holoenzyme complex. As before, it is unlikely that the two nucleotides interact at a single binding site as GTP is present at 100-fold excess concentration.

The concentration of ATP used in the above experiments (10–25 μM) suggests that AXP binding to the high-affinity ATPase catalytic site in gpA ($K_{\text{m,ATP}} \approx 5 \mu\text{M}$) negatively regulates GTP hydrolysis at a separate site, presumably a low-affinity NTPase catalytic site located in gpNu1 ($K_{\text{m,ATP}} \approx 470 \mu\text{M}$, $K_{\text{m,GTP}} \approx 500 \mu\text{M}$). Moreover, the data further

suggest that ATP hydrolysis at the high-affinity gpA catalytic site is stimulated by GXP binding to the low-affinity site in gpNu1. Finally, we note that while GTPase activity is strictly DNA-dependent, GXP-mediated stimulation of ATP hydrolysis does not require DNA. This suggests that while DNA is required for GTP *hydrolysis*, it is not required for GTP *binding*.⁴ The apparent K_D (136 μM) for GTP-mediated stimulation of ATPase activity may thus reflect GTP binding to the enzyme in the absence of catalytic turnover, yielding an estimate of the equilibrium constant for the formation of the binary terminase•GTP complex. That the apparent K_D for substrate (GTP) binding to the enzyme is lower than the K_m for catalytic turnover is common in enzyme-catalyzed reactions (26, 27).

Based on data available in the literature and those presented here, we propose the following model for communication between the NTPase catalytic sites in terminase holoenzyme (Figure 5). The gpA subunit of the enzyme contains a high-affinity ($K_m = 5 \mu\text{M}$) ATPase catalytic site while the gpNu1 subunit contains a low-affinity ($K_m \approx 500 \mu\text{M}$) NTPase catalytic site capable of binding and hydrolyzing either nucleotide. Thus, ATP binds to both enzyme subunits while GTP interacts only with gpNu1. DNA modulates the NTPase activity of gpNu1, stimulating ATP hydrolysis and critical to GTP hydrolysis. In the absence of DNA, GTP binds to the enzyme but is not hydrolyzed (panel A, Figure 5). In the presence of DNA, GTP turnover is observed. Binding of adenosine nucleotides to the gpA subunit negatively regulates the GTPase catalytic site in gpNu1, resulting in a decrease in the observed steady-state rate of GTP hydrolysis (panel A, Figure 5).

³ Our data do not rigorously exclude the possibility that both subunits of the enzyme possess GTPase catalytic sites but have identical K_m 's for GTP.

⁴ An alternate possibility is that a single catalytic turnover occurs on the enzyme, but that GDP release is extremely slow. In this model, DNA would stimulate GDP release from the enzyme, resulting in observable steady-state turnover.

ATP binding and hydrolysis occur at both enzyme subunits. GTP interacts with gpNu1 only and competes for ATP binding at that subunit (panel B, Figure 5). While it is expected that this would result in *inhibition* of ATP hydrolysis by the enzyme, binding of guanosine nucleotides to gpNu1 positively regulates the ATPase activity of the gpA subunit, resulting in an *increase* in the observed steady-state rate of ATP hydrolysis. This model predicts that adenosine and guanosine nucleotides can simultaneously bind to gpA and gpNu1, respectively, in the holoenzyme complex. Within this context, we note that ADP and GDP both stimulate the *cos*-cleavage reaction and that additive stimulation is observed. These data are consistent with the prediction that the dinucleotides can simultaneously bind to the enzyme, presumably at the separate binding sites in gpA and gpNu1, and suggest that NDP bound to each subunit independently stimulate nuclease activity.⁵

ATP plays multiple roles in phage λ terminase-mediated DNA packaging and virus assembly (Figure 1). The enzyme further possesses a DNA-dependent GTPase activity that plays an uncertain role in DNA packaging. While adenosine and guanosine nucleotides are equally effective in stimulating the *cos*-cleavage reaction, the effect of GXP on the fidelity of the reaction remains unknown. Earlier studies suggested that GTP supports the terminase-mediated strand-separation activity (16); however, work performed in our laboratory does not support this conclusion (12), and it is uncertain whether GXP performs this role *in vivo*. Finally, recent work has suggested that GTP does support, to some extent, the DNA translocase activity of the enzyme (16).

While the physiologic role of GTP in terminase-mediated virus assembly remains vague, the data presented here clearly demonstrate that the NTPase catalytic sites in the two enzyme subunits interact. Work in our laboratory has demonstrated negative hysteresis in the ATPase activity of λ terminase, and we have suggested that the ATP hydrolysis cycle in gpNu1 regulates the ATPase activity of the gpA subunit (L. Woods and C. E. Catalano, in preparation). These data provide further support for a model describing communication between the two ATPase catalytic sites in the terminase holoenzyme complex. We suggest that this communication is important in regulating the assembly and relative stability of the nucleoprotein packaging complexes (Figure 1), and coordinating the transitions between the multiple intermediates required for the assembly of an infectious virus.

⁵ An alternate possibility is that both nucleotides bind at the *same* site on the enzyme and that the apparent K_D for NDP binding to this site is relatively high. In this model, an increase in the "NDP" concentration results in increased occupation of the single NDP binding site on the enzyme and increased stimulation of nuclease activity. Given that each of the dinucleotides was included at a concentration of 1 mM, this model requires that the apparent K_D for NDP be >5 mM.

ACKNOWLEDGMENT

We thank Drs. Michael Feiss and Robert Kuchta for helpful discussions and critical review of the manuscript.

REFERENCES

1. Catalano, C. E., Cue, D., and Feiss, M. (1995) *Mol. Microbiol.* 16, 1075–1086.
2. Feiss, M. (1986) *Trends Genet.* 2, 100–104.
3. Becker, A., and Murialdo, H. (1990) *J. Bacteriol.* 172, 2819–2824.
4. Murialdo, H. (1991) *Annu. Rev. Biochem.* 60, 125–153.
5. Tomka, M. A., and Catalano, C. E. (1993) *J. Biol. Chem.* 268, 3056–3065.
6. Higgins, R. R., and Becker, A. (1995) *J. Mol. Biol.* 252, 31–46.
7. Shinder, G., and Gold, M. (1988) *J. Virol.* 62, 387–392.
8. Higgins, R. R., Lucko, H. J., and Becker, A. (1988) *Cell* 54, 765–775.
9. Higgins, R., and Becker, A. (1994) *EMBO J.* 13, 6152–6161.
10. Cue, D., and Feiss, M. (1993) *J. Mol. Biol.* 234, 594–609.
11. Woods, L., Terpening, C., and Catalano, C. E. (1997) *Biochemistry* 36, 5777–5785.
12. Yang, Q., and Catalano, C. E. (1997) *Biochemistry* 36, 10638–10645.
13. Tomka, M. A., and Catalano, C. E. (1993) *Biochemistry* 32, 11992–11997.
14. Hwang, Y., Catalano, C. E., and Feiss, M. (1996) *Biochemistry* 35, 2796–2803.
15. Hang, Q., Woods, L., Feiss, M., and Catalano, C. E. (1999) *J. Biol. Chem.* 274, 15305–15314.
16. Rubinchik, S., Parris, W., and Gold, M. (1994) *J. Biol. Chem.* 269, 13586–13593.
17. Meyer, J. D., Hanagan, A., Manning, M. C., and Catalano, C. E. (1998) *Int. J. Biol. Macromol.* 23, 27–36.
18. Nash, H. A., Robertson, C. A., Flamm, E., Weisberg, R. A., and Miller, H. I. (1987) *J. Bacteriol.* 169, 4124–4127.
19. Yang, Q., Hanagan, A., and Catalano, C. E. (1997) *Biochemistry* 36, 2744–2752.
20. Cue, D., and Feiss, M. (1992) *J. Mol. Biol.* 228, 58–71.
21. Rubinchik, S., Parris, W., and Gold, M. (1994) *J. Biol. Chem.* 269, 13575–13585.
22. Yang, Q., Berton, N., Manning, M. C., and Catalano, C. E. (1999) *Biochemistry* (in press).
23. Bear, S., Court, D., and Friedman, D. (1984) *J. Virol.* 52, 966–972.
24. Becker, A., and Gold, M. (1978) *Proc. Natl. Acad. Sci. U.S.A.* 75, 4199–4203.
25. Parris, W., Rubinchik, S., Yang, Y.-C., and Gold, M. (1994) *J. Biol. Chem.* 269, 13564–13574.
26. Stryer, L. (1995) *Biochemistry*, Fourth ed., W. H. Freeman and Co., New York.
27. Fersht, A. (1985) *Enzyme Structure and Mechanism*, 2nd ed., W. H. Freeman and Co., New York.

BI990866L